Ni-catalysed acceptorless dehydrogenative aromatisation of cyclohexanone derivatives enabled by concerted catalysis specific to supported nanoparticles

Takehiro Matsuyama,[1] Takafumi Yatabe,[1,2]* Tomohiro Yabe,[1] and Kazuya Yamaguchi[1]*

[1]Department of Applied Chemistry, School of Engineering, The University of Tokyo, 7-3-1 Hongo, Bunkyo-ku, Tokyo 113-8656, Japan.

[2]Precursory Research for Embryonic Science and Technology (PRESTO), Japan Science and Technology Agency (JST), 4-1-8 Honcho, Kawaguchi, Saitama 332-0012, Japan.

*e-mail: kyama@appchem.t.u-tokyo.ac.jp, yatabe@appchem.t.u-tokyo.ac.jp

Abstract

The dehydrogenative aromatisation of cyclohexanone derivatives has had a transformative influence on the synthesis of aromatic compounds because functional groups can be easily introduced at desired positions via classic organic reactions without being limited by *ortho*-, *meta*- or *para*-orientations. However, research is still limited on acceptorless dehydrogenative aromatisation, especially with regard to nonprecious-metal catalysts. Ni is a promising candidate catalyst as a congener of Pd, but thermally Ni-catalysed dehydrogenative aromatisation has not been reported even in an oxidative manner because of the difficulty of β-hydride elimination and the fast re-insertion of Ni–H species. Here, we report a CeO_2-supported Ni(0) nanoparticle catalyst for acceptorless dehydrogenative aromatisation of cyclohexanone derivatives. This catalyst is widely applicable to various compounds such as cyclohexanols, cyclohexylamines, *N*-heterocycles, enamines and *N*-alkyl piperidones. Through various experiments, we demonstrate that the present reaction was achieved by the concerted catalysis utilizing metal ensembles unique to supported metal nanoparticle catalysts.

Graphical Abstract

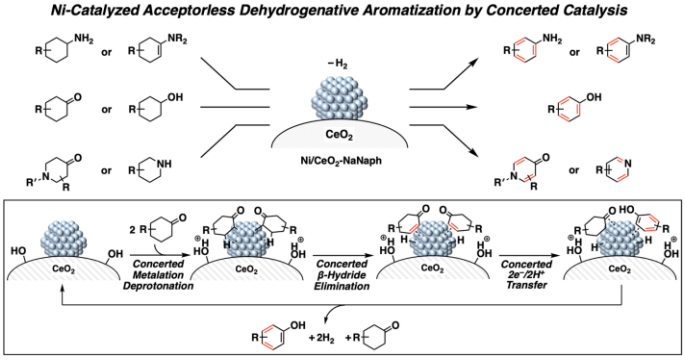

Introduction

Metal ensembles of nanoparticles exhibit a catalytic performance distinct from that of mononuclear complexes because the substrates and intermediates can be activated or adsorbed on multiple active sites of the metal nanoparticles in a unique fashion[1–4]. For example, in 2021, Ordomsky et al.[4] reported a novel strategy for size-dependent selective hydrogenation using molecularly imprinted Pd nanoparticle catalysts, which they prepared via poisoning of the Pd surface except for positions adsorbed by template molecules such as benzene. This selectively catalysed hydrogenation of aromatic compounds with the same size as the template molecules. In addition, combining metal nanoparticles with appropriate supports realises a synergistic catalysis that efficiently promotes the desired reaction while enhancing the stability of the active species[5–8].

Aromatic compounds are a ubiquitous building block in various fields, and many efforts have been made to establish methodologies for their synthesis. In general, substituted aromatic compounds are synthesised via classic nucleophilic aromatic substitution (S_NAr) or electrophilic aromatic substitution (S_EAr), but the regioselectivity is constrained by the substituents[9,10]. Although cross-coupling and C–H functionalisation have been used to realise regioselective synthesis, inherent problems remain such as regioselectivity control of prefunctionalisation, generation of toxic (pseudo-)halogenated products and the requirement for directing groups[11–13]. As an alternative approach, in 2011, Stahl et al.[14] reported synthesising phenols from nonaromatic cyclohexanones via Pd-catalysed aerobic dehydrogenative aromatisation, where the substituents are easily introduced regioselectively in any position by classic organic reactions[15]. Since then, catalytic dehydrogenative aromatisation has been applied to synthesising various kinds of substituted aromatic hydrocarbons including phenols, anilines and ethers (Fig. 1a)[16–19].

Dehydrogenative aromatisation is classified into two types: oxidative or acceptorless[16–19]. Most reports on dehydrogenative aromatisation have been on the oxidative type, which mainly utilised Cu- or Pd-based catalysts or transition-metal-free systems. Research on acceptorless dehydrogenative aromatisation is scarce despite the high atom economy, where H_2 is the sole theoretical by-product in the case of phenol synthesis (Fig. 1a). Liu et al.[20] reported the first example of liquid-phase acceptorless dehydrogenative aromatisation of cyclohexanones to phenols using Pd/C. Since then, other groups, including ours, have also reported synthesising aromatic compounds by combining acceptorless dehydrogenative aromatisation with condensation between nucleophiles or electrophiles and cyclohexanones in the presence of Pd-based catalysts[21–28]. Although noble-metal catalysts like Pd have been widely applied to acceptorless dehydrogenation[29–31] as exemplified by such aromatisation reactions, their high cost and limited supply have increased demand for alternative approaches that

use nonprecious-metal catalysts. In recent years, acceptorless dehydrogenation through hydrogen atom transfer (HAT), which utilises both photoredox catalysts and transition-metal catalysts including non-precious ones, has attracted much attention because of its high site selectivity and mild reaction conditions (Fig. 1b)[15,32–37]. However, the reported photocatalytic systems for acceptorless dehydrogenative aromatisation typically require activated cyclohexane skeletons possessing benzylic, allylic or heteroatom-neighbouring C–H bonds, which have relatively low bond dissociation energies (BDEs) (Fig. 1b)[15,34–36]. Quite recently, Kanai et al.[37] posted acceptorless dehydrogenative aromatisation of cycloalkanes without requiring the aforementioned weak C–H bonds based on dual HAT strategy by utilizing photoredox catalysis, but this report did not apply to dehydrogenative aromatisation of cyclohexanones to afford phenols. To the best of our knowledge, nonprecious-metal catalysts have never been applied to the acceptorless dehydrogenative aromatisation of cyclohexanones without possessing such C–H bonds whose BDEs are low.

Previous reports on acceptorless dehydrogenative aromatisation have mainly used Pd-based catalysts. Ni is a congener of Pd, and thus, we considered it as a promising nonprecious-metal candidate for catalysing acceptorless dehydrogenative aromatisation. However, no Ni-based catalysts have been reported for dehydrogenative aromatisation without photoirradiation, even for the oxidative type. Using Ni-based catalysts to achieve acceptorless dehydrogenative aromatisation has several challenges compared with well-known Pd-based catalysts. First, the activation energy of β-hydride elimination to afford alkenes is higher in Ni-alkyl intermediates than in Pd-based counterparts because the lower electronegativity of Ni weakens the agostic interactions between Ni and H species at the β-position and because its smaller atomic radius renders the transition state more unstable due to geometrical limitations (Fig. 1c)[38–41]. Second, the fast migratory insertion of hydride species on the Ni centre into alkene species[42–44] before H_2 evolution inhibits the formation of dehydrogenated products (Fig. 1c). Finally, the Ni-based catalyst needs to be sufficiently stable to function even at high temperatures because acceptorless dehydrogenative aromatisation is more thermodynamically unfavourable than oxidative aromatisation.

Herein, we have developed acceptorless dehydrogenative aromatisation of cyclohexanones to phenols by utilizing a multifunctional CeO_2-supported Ni(0) nanoparticle heterogeneous catalyst prepared via reduction using sodium naphthalenide (Ni/CeO_2-NaNaph). Unprecedented Ni-catalysed dehydrogenative aromatisation was enabled by the following features (Fig. 1d):

- The concerted metalation deprotonation of cyclohexanones to Ni(0) nanoparticles with the assistance of Brønsted base sites in the CeO_2 support without the addition of external bases,

- The concerted β-hydride elimination to form cyclohexenones and Ni–H species on multiple active sites of Ni nanoparticles to overcome the aforementioned disadvantages derived from its smaller atomic radius for β-hydride elimination and
- The concerted two-electron/two-proton transfer from one cyclohexenone to another cyclohexenone (fast disproportionation of cyclohexenones) to form phenols and cyclohexanones enabled by their simultaneous adsorption on the surface of Ni nanoparticles, which inhibits the re-insertion of hydride species from the Ni–H species to cyclohexenones, followed by H_2 evolution from the Ni–H species on Ni nanoparticles and protons on CeO_2.

This system was also applicable to acceptorless dehydrogenation of various compounds such as cyclohexanols, cyclohexylamines, *N*-heterocycles, enamines, and *N*-alkyl piperidones. We thoroughly performed catalyst characterisation, kinetic analyses and control experiments to demonstrate the unique performance of the prepared catalytic system and to compare it to other catalysts.

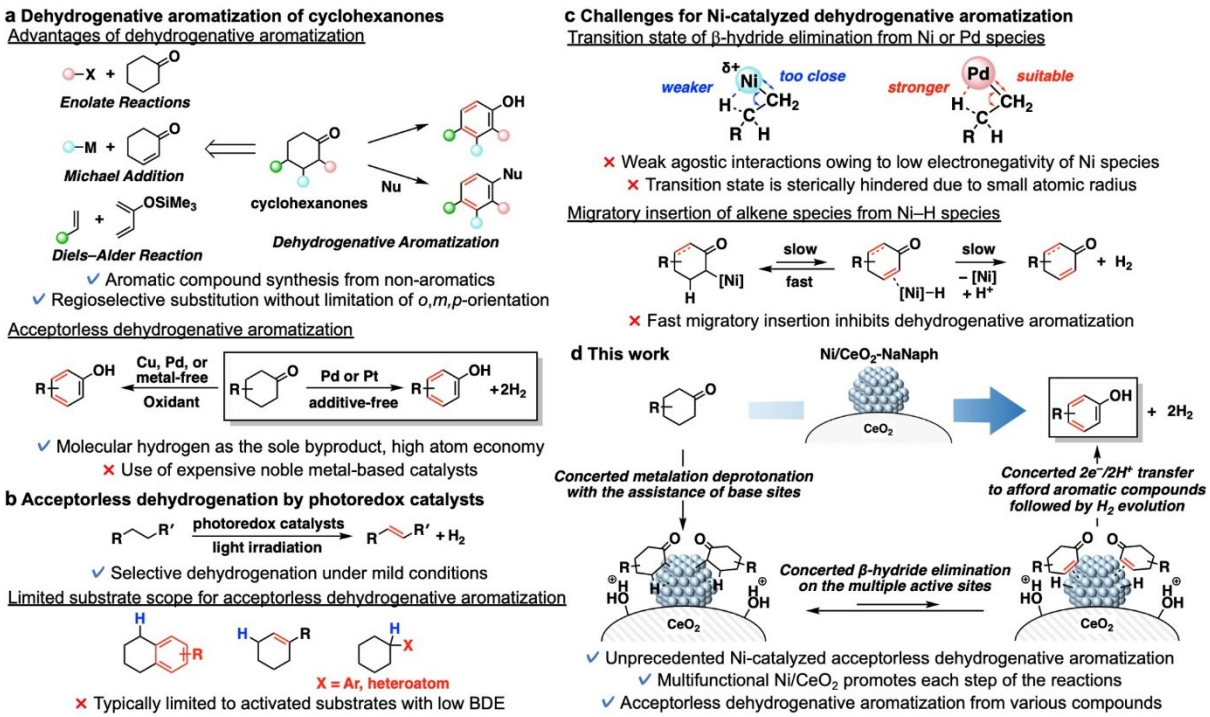

Fig. 1: Background and overview of the study. a, Advantages and types of dehydrogenative aromatisation of cyclohexanones. **b,** Acceptorless dehydrogenation by photoredox catalysts. **c,** Challenges for Ni-catalysed dehydrogenative aromatisation. **d,** This work: First example of Ni-catalysed acceptorless dehydrogenative aromatisation of various compounds including cyclohexanones facilitated by concerted catalysis utilizing the metal ensembles and support basicity of Ni/CeO_2-NaNaph.

Results

Catalyst characterisation

Ni/CeO_2-NaNaph was prepared as described in our previous report with some modifications[45,46]. Briefly, a CeO_2-supported Ni hydroxide precursor ($Ni(OH)_x/CeO_2$) prepared via deposition–precipitation was reduced by sodium naphthalenide (NaNaph) in tetrahydrofuran (THF) at room temperature (~24 °C) in an Ar atmosphere to afford Ni/CeO_2-NaNaph (Ni: 1.38 wt%). The Ni K-edge X-ray absorption near-edge structure (XANES) spectrum of Ni/CeO_2-NaNaph was between those of Ni foil and $Ni(OH)_2$, which indicates that most Ni species in Ni/CeO_2-NaNaph were zero-valent. According to linear combination fitting (LCF), ~76% of the Ni species were zero-valent (Fig. 2a; Supplementary Fig. 1a). This is mostly consistent with the X-ray photoelectron spectroscopy (XPS) results (Fig. 2b; Supplementary Fig. 2, Supplementary Table 1). The k^3-weighted Fourier-transformed Ni K-edge-extended X-ray absorption fine-structure (EXAFS) spectrum of Ni/CeO_2-NaNaph exhibited scattering originated from Ni−Ni bond of Ni metal in the first coordination sphere while very weak counterparts in the second coordination sphere were observed, suggesting the presence of highly dispersed Ni(0) species in Ni/CeO_2-NaNaph (Fig. 2c; Supplementary Fig. 3, Supplementary Table 2). In fact, the diffuse reflectance infrared Fourier transform (DRIFT) spectrum of CO adsorbed on Ni/CeO_2-NaNaph exhibited a peak around 2050 cm^{-1}, which could be assigned to linear CO species adsorbed on zero-valent Ni species, but bridged species were not observed (Fig. 2d)[47]. Although direct observation of Ni species supported on CeO_2 by high-angle annular dark-field scanning transmission electron microscopy (HAADF-STEM) was difficult (Fig. 2e), STEM-energy-dispersive spectroscopy (EDS) mapping confirmed that highly dispersed Ni species were supported on CeO_2 (Fig. 2f, 2g). The X-ray diffraction (XRD) patterns of Ni/CeO_2-NaNaph were comparable with those of CeO_2 and $Ni(OH)_x/CeO_2$, which supports that Ni(0) species were successfully immobilised on CeO_2 with the CeO_2 structures intact (Fig. 2h).

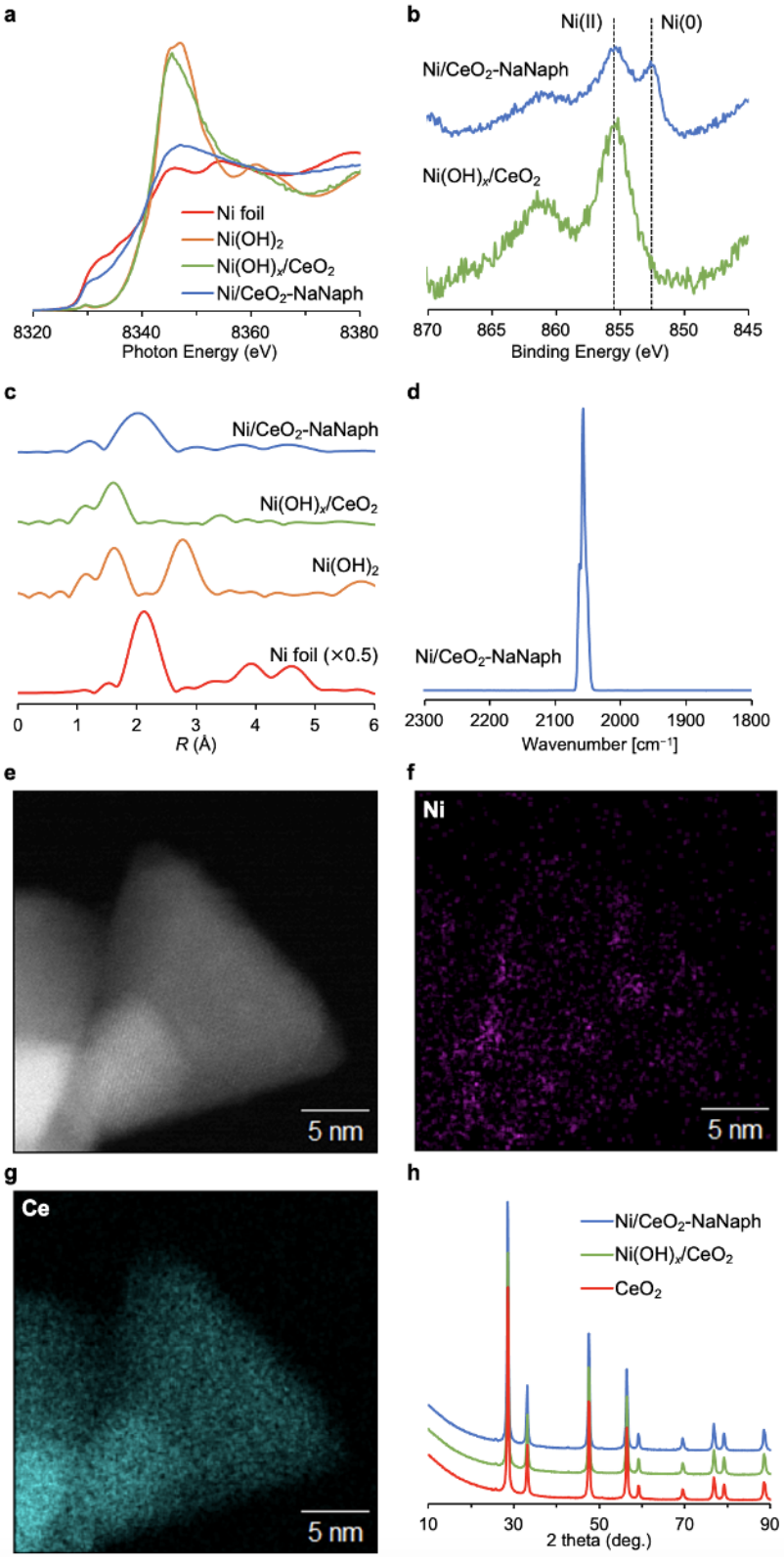

Fig. 2: Characterisation of Ni catalysts. a, Ni K-edge XANES spectra. **b,** Ni 2p XPS spectra. **c,** k^3-weighted Fourier-transformed Ni K-edge EXAFS spectra. **d,** DRIFT spectrum of CO adsorbed on Ni/CeO_2-NaNaph. **e,** HAADF-STEM image of Ni/CeO_2-NaNaph. STEM-EDS mappings of Ni/CeO_2-NaNaph showing the distributions of **f,** Ni (magenta) and **g,** Ce (cyan). **h,** XRD patterns.

Catalyst effect

We initially investigated the effect of supported nonprecious-metal nanoparticle catalysts on acceptorless dehydrogenative aromatisation using 4-methylcyclohexanone (**1a**) as a model substrate under the reaction conditions indicated in Table 1. With Ni/CeO_2-0.3NaNaph (prepared in the same manner as in our previous report[45] by using 0.3 equivalent of NaNaph to the amount of NaNaph used to prepare Ni/CeO_2-NaNaph), the desired dehydrogenated product *p*-cresol (**2a**) was obtained with a 50% yield along with 2-methylated phenol (**2a′**) with a 2% yield (Table 1, entry 1) (**2a′** formation mechanism was discussed in the Supplementary Information). Interestingly, other supported 3d-transition-metal nanoparticle catalysts including Cu, Co, Mn, Fe and Zn did not catalyse dehydrogenative aromatisation (Table 1, entries 2–6). The Ni loading did not greatly affect dehydrogenative aromatisation (Supplementary Table 3). However, the yield of **2a** was slightly improved by increasing the amount of reducing reagent to prepare Ni/CeO_2-NaNaph (Table 1, entry 7). Next, we investigated the effect of the supports at 180°C. Only Ni/CeO_2-NaNaph exhibited a high catalytic performance to afford **2a** with a 74% yield (Table 1, entry 8). Ni catalysts on other supports such as hydroxyapatite (HAP), ZrO_2, TiO_2 and Al_2O_3 hardly catalysed the reaction (Table 1, entries 9–12). In addition, as-purchased CeO_2, CeO_2 reduced by NaNaph (CeO_2-NaNaph) and Ni$(OH)_x$/CeO_2 did not catalyse the reaction (Table 1, entries 13–15). These results indicate that the reduced Ni was the actual active species. The solvent was also shown to have a substantial effect, and the yield of **2a** was highest when *N*,*N*-dimethylacetamide (DMA) was used as the solvent (Supplementary Table 4). Dehydrogenative aromatisation of 3,5-dimethylcyclohexanone (**1g**) was immediately stopped by hot filtration of Ni/CeO_2-NaNaph (Supplementary Fig. 4), and inductively coupled plasma atomic emission spectroscopy (ICP-AES) showed that almost no Ni species were in the filtrate (Ni: 0.21% of the Ni species used for the reaction), which indicates that the observed catalysis was heterogeneous.

To clarify the effect of the supports, Ni/CeO_2-NaNaph was compared with Ni/HAP-NaNaph. The k^3-weighted Ni K-edge EXAFS spectrum of Ni/CeO_2-NaNaph exhibited very weak scattering originating from the Ni–Ni bond in the second coordination sphere whereas that of Ni/HAP-NaNaph exhibited relatively strong scattering (Supplementary Fig. 5, Supplementary Table 2). These results indicate the presence of ultrasmall Ni(0) nanospecies in the Ni/CeO_2-NaNaph, which was likely due to the strong interaction between Ni(0) nanospecies and CeO_2[45]. Then, the effect of the basicity of the supports on dehydrogenative aromatisation was investigated. Dehydrogenative aromatisation of **1a** was completely suppressed in the presence of benzoic acid (PhCOOH) (Table 1, entry 16). Meanwhile, dehydrogenative aromatisation of **1a** using Ni/HAP-NaNaph was promoted by the addition of CeO_2-NaNaph and Na_2CO_3, which indicates that the basicity of CeO_2 promoted the deprotonative

metalation step (Table 1, entries 17–19). Thus, the exceptional catalytic activity of Ni/CeO_2-NaNaph for dehydrogenative aromatisation can be attributed to the high dispersion of Ni(0) species induced by strong interaction with CeO_2 and the synergistic catalysis between Ni(0) species and the basic sites of CeO_2.

Substrate scope

Next, we evaluated the substrate scope of Ni/CeO_2-NaNaph for catalysing acceptorless dehydrogenative aromatisation of cyclohexanones (**1**) to phenols (**2**) (Fig. 3, **2a**–**2q** from cyclohexanones; see Supplementary Table 5 for the detailed information on the by-products in substrate scope investigation). This catalytic system is applicable to *para*-, *meta*- and *ortho*-methyl-substituted phenol synthesis (**1a**–**1c**). Other alkyl-substituted cyclohexanones including 4-ethyl- (**1d**), 4-propyl- (**1e**), 3,4-dimethyl- (**1f**), 3,5-dimethyl- (**1g**) and 4-*tert*-butyl- (**1h**) ones were successfully converted into the corresponding phenols with good to moderate yields. This system could also be applied to the dehydrogenative aromatisation of aryl-substituted cyclohexanones (**1i**, **1j**). In the case of cyclohexanones with various functional groups such as acetal, ethyl ester and acetamide, this catalytic system worked well at affording the desired dehydrogenated products with the functional groups intact (**1k**–**1m**). In addition, 1-tetralone (**1n**) and 1,4-cyclohexanedione (**1o**) were converted into corresponding phenols with good yields. Cyclohexenones such as 3-methyl-2-cyclohexen-1-one (**1p**) and carvone (**1q**) could be subjected to dehydrogenative aromatisation, but the C=C bond in the corresponding phenol obtained from carvone was hydrogenated.

Several studies have reported on the acceptorless dehydrogenation of secondary alcohols to afford the corresponding ketones in the presence of supported Ni nanoparticle catalysts[48,49], which motivated us to investigate acceptorless dehydrogenative aromatisation of cyclohexanols (**3**) to phenols (**2**). Cyclohexanol is commercially obtained as ketone–alcohol (K–A) oil via hydrogenation of benzene followed by aerobic cyclohexane oxidation. Thus, if H_2 formed by acceptorless dehydrogenative aromatisation of cyclohexanol is retrieved and used for benzene hydrogenation, then a formal process of aerobic benzene oxidation to phenol could be constructed[21]. As expected, 4-methylcyclohexanol (**3a**) was successfully converted into the corresponding phenol (**2a**) with a good yield in the presence of Ni/CeO_2-NaNaph while a CeO_2-supported Pd nanoparticle catalyst (Pd/CeO_2-NaNaph) produced **2a** with a much lower yield (Supplementary Table 6). This is because Pd nanoparticles hardly catalyse the dehydrogenation of cyclohexanols to cyclohexanones. The substrate scope of the catalytic system for dehydrogenative aromatisation starting from cyclohexanols (Fig. 3, **2a**–**2d**, **2f**–**2h**, **2n**, **2o** from cyclohexanols) includes various alkyl-substituted cyclohexanols (**3a**–**3d**, **3f**–**3h**). In addition, 1,2,3,4-

tetrahydro-1-naphthol (**3n**) and 1,4-cyclohexanediol (**3o**) were efficiently converted into phenols.

We found that Ni/CeO_2-NaNaph could also catalyse the acceptorless dehydrogenative aromatisation of cyclohexylamines (**4a**–**4d**) to afford primary anilines (Fig. 3, **5a**–**5d**), enamines (**6a**–**6c**) to afford aryl amines (Fig. 3, **7a**–**7d**) and *N*-heterocycles (**8a**–**8d**) (Fig. 3, **9a**–**9d**). With regard to dehydrogenative aromatisation for enamines, using Ni/CeO_2-NaNaph to catalyse dehydrogenative aromatisation from 1-morpholino-cyclohexene (**6a**) resulted in the gradual formation of a dehydrogenated product (**7a**) via sequential dehydrogenation (Supplementary Fig. 6a) to achieve a high yield of **7a** (Fig. 3), whereas using Pd/CeO_2-NaNaph as the catalyst produced **7a** and the hydrogenated product (**7a′**) at a ratio of 1:2 immediately after the reaction was started due to the disproportionation of **6a** on Pd nanoparticles[50] (Supplementary Fig. 6b), which resulted in a moderate yield of **7a** even after 24 h (Supplementary Fig. 7). Then, Ni/CeO_2-NaNaph-catalysed α,β-dehydrogenation of *N*-alkyl piperidones (**10a**–**10c**) was conducted (Fig. 3, **11a**–**11c**), which surprisingly selectively converted 1-methyl-4-piperidone (**10a**) into 1-methyl-4(*1H*)-pyridinone (**11a**) with an excellent yield via double dehydrogenation of **10a**. This reaction has not previously been reported. The reactions from 1-methyl-4-piperidone with a methyl group at the α-position of the carbonyl group (**10b**) and 1-ethyl-4-piperidone (**10c**) were successful, and they afforded corresponding double-dehydrogenated products with good yields.

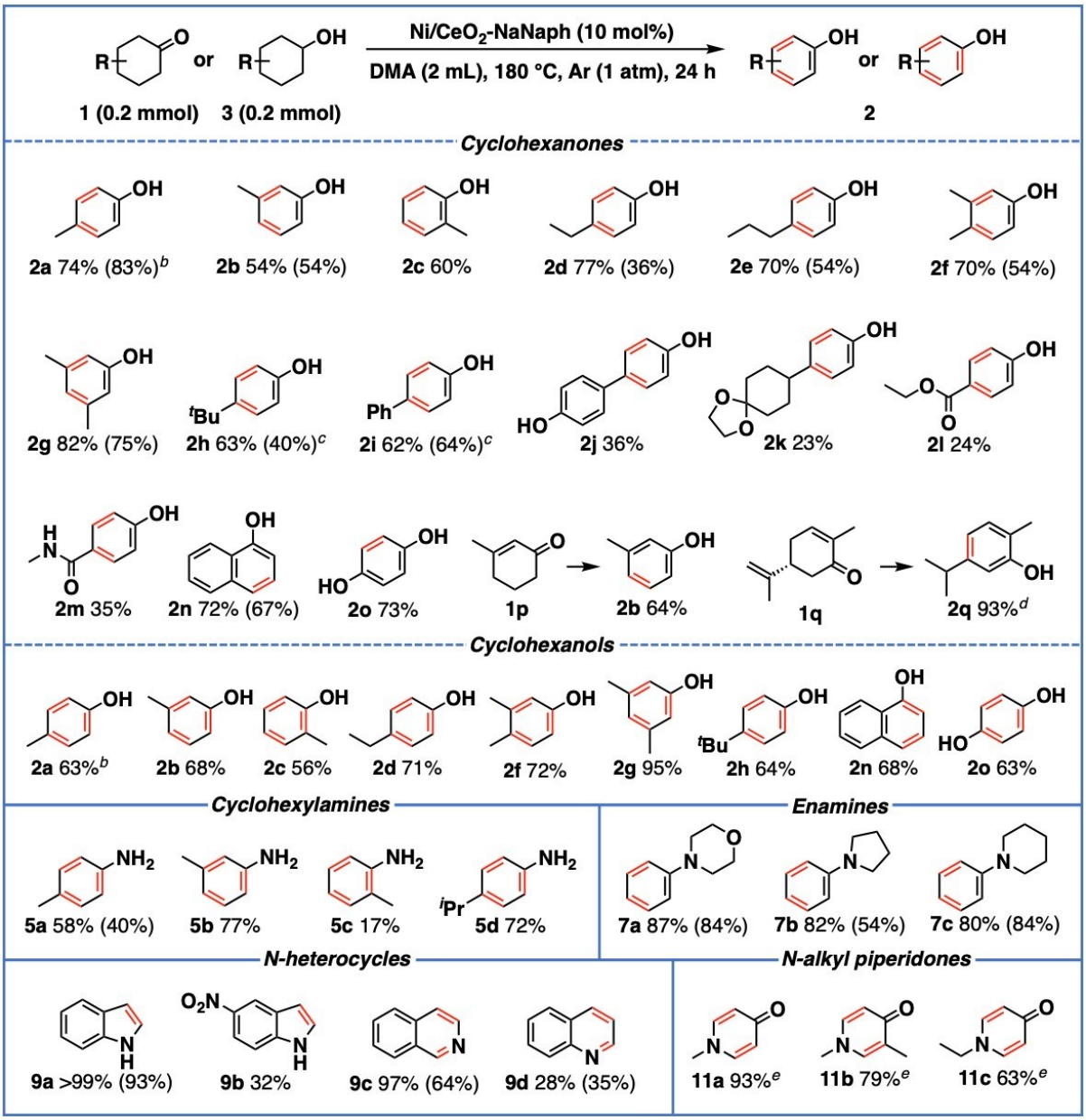

Fig. 3: Substrate scope for acceptorless dehydrogenation of cyclohexanones, cyclohexanols, cyclohexylamines, *N*-heterocycles, enamines and *N*-alkyl piperidones.[a] [a] Reaction conditions: **1**, **3**, **4**, **6** or **8** (0.2 mmol), Ni/CeO_2-NaNaph (Ni: 10 mol%), DMA (2 mL), Ar (1 atm), 180°C, 24 h. Yields were determined by GC analysis using *n*-hexadecane as an internal standard. Values in parentheses are isolated yields. [b] **1** or **3** (0.3 mmol), Ni/CeO_2-NaNaph (Ni: 3.3 mol%). [c] **1** (0.3 mmol), Ni/CeO_2-NaNaph (Ni: 10 mol%). [d] Yield of the intramolecular disproportionated product is shown. [e] **10** (0.3 mmol), Ni/CeO_2-NaNaph (Ni: 3.3 mol%), 1,4-dioxane (2 mL), 120°C.

Mechanistic studies

To confirm that the dehydrogenative aromatisation proceeded without any hydrogen acceptors, gas chromatography (GC) was used to analyse the gas phase after dehydrogenative aromatisation of **1g** (Supplementary Fig. 8). The results showed approximately two equivalents of H_2 to the dehydrogenated product (**2g**), which indicates that the dehydrogenative aromatisation was the acceptorless type. In addition, when 3-methyl-2-cyclohexen-1-one (**1p**) was the substrate, *m*-cresol (**2b**) and 3-methylcyclohexanone (**1b**) were produced with almost the same yields 10 min after the reaction was started (Supplementary Fig. 9). Together with the above results on support effects and our previous reports on acceptorless dehydrogenative aromatisation by supported Pd nanoparticle catalysts[21–27,50,51], we propose the following mechanism for the formation of phenols from cyclohexanones (Supplementary Fig. 10): (1) cyclohexanones adsorb onto the surface of Ni nanoparticles; (2) cyclohexanones undergo concerted metalation deprotonation to Ni species with the assistance of Brønsted base sites in CeO_2; (3) β-hydride elimination takes place to afford cyclohexenones; (4) cyclohexenones undergo disproportionation to afford phenols and cyclohexanones on the surface of the Ni nanoparticles and (5) H_2 evolution occurs to achieve the catalytic cycle.

A series of kinetic analyses were conducted to determine the turnover-limiting step. We confirmed that the initial rate for the dehydrogenative aromatisation of cyclohexanone (**1r**) was saturated to the initial substrate concentrations under normal conditions in the present catalytic system (Supplementary Fig. 11), which indicates that the adsorption of **1r** to Ni species was not the turnover-limiting step. The **2b** production rate using **1p** as the starting material was much higher than that using **1b** (Supplementary Fig. 12), which indicates that the disproportionation of cyclohexenones was not the turnover-limiting step. The kinetic isotope effect (KIE) was not observed when **1r** and cyclohexanone-α-d_4 (**1r**-α-d_4, k_H/k_{D4} = 1.1) were used, which indicates that deprotonative metalation and H_2 evolution were not the turnover-limiting steps (Fig. 4a). In contrast, KIE was observed when **1r**-α-d_4 and cyclohexanone-d_{10} (**1r**-d_{10}, k_{D4}/k_{D10} = 2.3) were used (Fig. 4a). These results indicate that the turnover-limiting step of Ni/CeO_2-NaNaph-catalysed dehydrogenative aromatisation is β-hydride elimination. On the other hand, in the presence of Pd/CeO_2-NaNaph, KIE was observed with **1r** and **1r**-α-d_4 (k_H/k_{D4} = 2.6) but not with **1r**-α-d_4 and **1r**-d_{10} (k_{D4}/k_{D10} = 1.3) (Fig. 4b), which indicates that the turnover-limiting step of Pd/CeO_2-NaNaph-catalysed dehydrogenative aromatisation is the deprotonative metalation of cyclohexanones.

We conducted various control experiments to elucidate why our catalytic system enabled unprecedented Ni-catalysed acceptorless dehydrogenative aromatisation. First, we compared Ni/CeO_2-NaNaph with other Ni complex catalysts for the dehydrogenative aromatisation of **1a** (Supplementary Table 7). While **2a** was not

produced in the presence of Ni(II) complexes (Supplementary Table 7, entries 1–4), some **2a** was produced when $Ni(cod)_2$ and IPr (1,3-bis(2,6-diisopropylphenyl)imidazol-2-ylidene) (Ni-IPr complex) were used (Table 1, entry 20). To clarify which steps were difficult for the Ni complexes, several experiments using deuterium-labeled cyclohexanones were conducted. The H/D exchange of **1r**-α-d_4 efficiently proceeded 12 h after dehydrogenative aromatisation was started in the presence of the Ni-IPr complex (Fig. 4c), whereas the use of either $Ni(cod)_2$ or IPr caused the H/D exchange of **1r**-α-d_4 to hardly proceed under the same reaction conditions (Supplementary Fig. 13). Thus, α-C–H activation of **1r** could occur with the Ni-IPr complex. However, the GC-MS and ^{2}H NMR spectra of **1r**-β,γ-d_6 (deuteration rate of α-position = 4%) after stirring with the Ni-IPr complex at 160°C for 12 h were comparable to those before stirring, which indicates that a decrease in D from **1r**-β,γ-d_6 or H/D scrambling between the α- and β-positions via β-hydride elimination followed by insertion did not occur (Fig. 4d; Supplementary Figs. 14–16). These results indicate that β-hydride elimination was difficult to induce in the case of Ni complexes. Based on these results and the different turnover-limiting steps of Ni nanoparticles and Pd nanoparticles, we concluded that Ni species generally have difficulty with β-hydride elimination because of their smaller atomic radius compared with Pd species[38–41], but the concerted catalysis by multiple active sites (Ni–Ni metal ensembles) of Ni nanoparticles could help attenuate the steric restriction and facilitate β-hydride elimination, which explains how our catalytic system achieved the unprecedented Ni-catalysed dehydrogenative aromatisation (Supplementary Fig. 17).

As noted earlier, when **1p** was used as the starting material, fast disproportionation occurred to afford **2b** and **1b** in the presence of Ni/CeO_2-NaNaph. However, the Ni-IPr complex hardly catalysed the reaction (Fig. 4e). Considering the different mechanisms of Pd mononuclear active sites and Pd nanoparticles for dehydrogenative aromatisation to phenols[51,52], such a fast disproportionation of cyclohexenones to phenols and cyclohexanones appears specific to metal nanoparticle catalysts. This may be because the disproportionation proceeds via a concerted two-electron/two-proton transfer from one cyclohexenone to another cyclohexenone after the two cyclohexenone molecules adsorb together on metal nanoparticles with the metal ensembles (Supplementary Fig. 18). Furthermore, acceptorless dehydrogenation of 4,4-dimethylcyclohexanone (**1s**), which affords nonaromatic dehydrogenated products even after double dehydrogenation, did not proceed with Ni/CeO_2-NaNaph, but small amounts of the corresponding dehydrogenated products 4,4-dimethylcyclohexa-2,5-dien-1-one (**2s**) and 4,4-dimethylcyclohex-2-en-1-one (**2s″**) formed in the presence of Pd/CeO_2-NaNaph (Fig. 4f). Based on the facileness of migratory insertion of Ni–H species to olefins compared with that of Pd–H species[42–44], these results indicate that the re-insertion of Ni–H species produced by β-hydride elimination of **1s** to **2s″** occurs faster than H_2

evolution, which explains the lack of dehydrogenated products from **1s** with Ni/CeO_2-NaNaph. Therefore, the fast disproportionation of cyclohexenones via the concerted two-electron/two-proton transfer on Ni nanoparticles to produce phenols, which are difficult to insert into Ni–H species, is another key factor for how we achieved Ni-catalysed acceptorless dehydrogenative aromatisation.

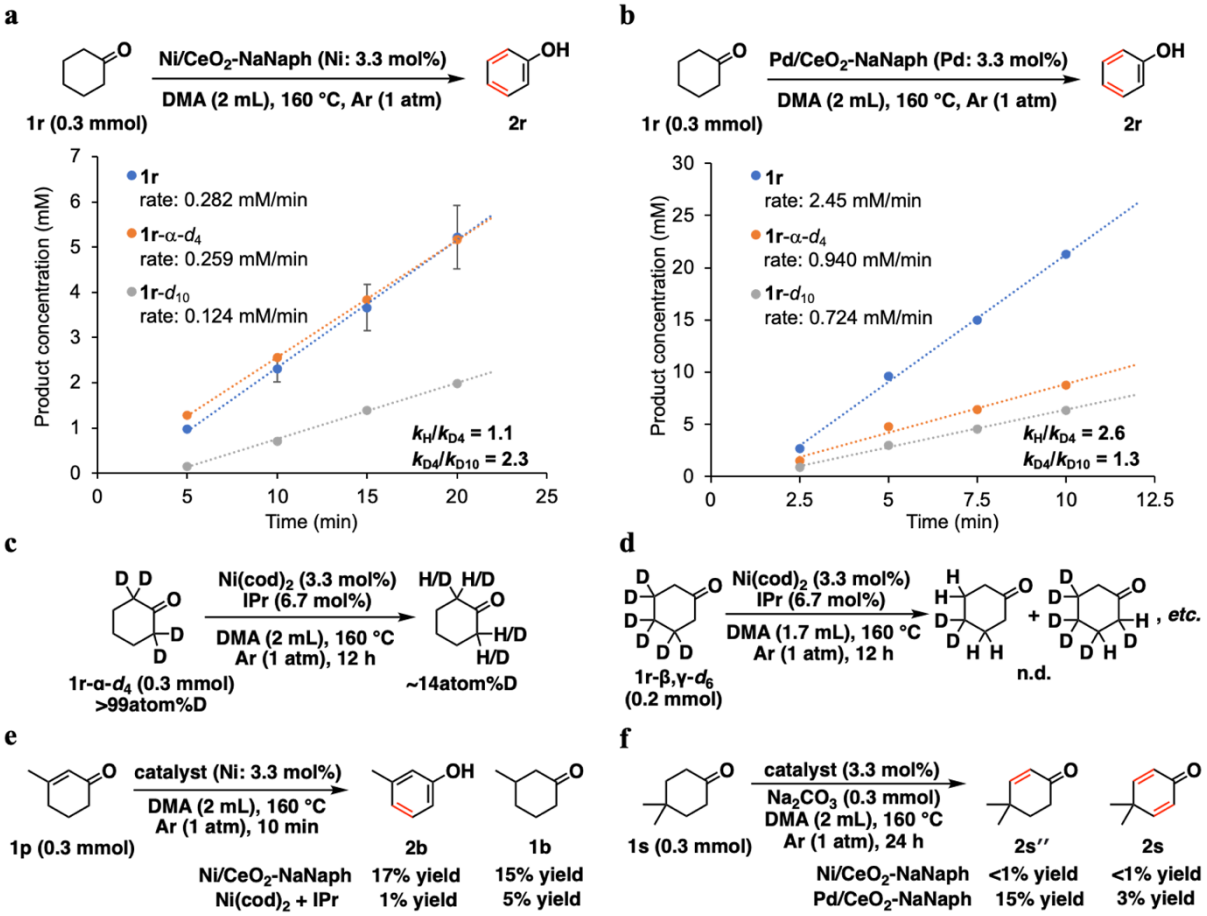

Fig. 4: Kinetic analyses and control experiments. Kinetic isotope effect on acceptorless dehydrogenative aromatisation of **1r** in the presence of **a,** Ni/CeO_2-NaNaph or **b,** Pd/CeO_2-NaNaph. **c,** H/D exchange of **1r**-α-d_4 in the presence of the Ni-IPr complex. **d,** H/D exchange of **1r**-β,γ-d_6 in the presence of the Ni-IPr complex. **e,** Ni/CeO_2-NaNaph- or Ni-IPr-catalysed disproportionation of **1p**. **f,** Acceptorless dehydrogenation of **1s** in the presence of Ni/CeO_2-NaNaph or Pd/CeO_2-NaNaph. Note: n.d. = not detected.

Conclusion

We demonstrated the first example of Ni-catalysed acceptorless dehydrogenative aromatisation of cyclohexanones via α,β-dehydrogenation. Our CeO_2-supported Ni(0) nanoparticle catalyst is applicable to the acceptorless dehydrogenation of various substrates including cyclohexanols, cyclohexylamines, *N*-heterocycles, enamines and *N*-alkyl piperidones. The results of our catalyst characterisation, kinetic analyses and control experiments showed that Ni/CeO_2-NaNaph is a multifunctional catalyst that exhibits the concerted catalysis utilizing metal ensembles and support basicity to promote each step of acceptorless dehydrogenative aromatisation. Our results show how the unique active site structures of supported nanoparticle catalysts compared to those of mononuclear complexes effectively facilitate organic reactions. We expect that our findings will contribute to the development of novel molecular transformations using supported nanoparticle catalysts in the future.

Methods

Preparation of Ni/CeO_2-NaNaph

First, $Ni(OH)_x/CeO_2$ was prepared as the precursor according to the following method. The aqueous solution (60 mL) of $NiCl_2 \cdot 6H_2O$ (118.8 mg, 8.3 mM) with CeO_2 (2.0 g), which was calcinated in the air at 550 °C for 3 h, was vigorously stirred at room temperature. After 15 min, the pH of the solution was adjusted to 11.0 by addition of an aqueous solution of NaOH (1.0 M), and the resulting slurry was stirred overnight. The solid was then filtered off, washed with a large amount of water (3 L) and dried to afford 2.0 g of $Ni(OH)_x/CeO_2$ as a pale yellow powder. $Ni(OH)_x/CeO_2$ was stored in an Ar-filled glove-box after being heated at 150 °C for 15 min *in vacuo*.

Then, Ni/CeO_2-NaNaph was prepared as follows. $Ni(OH)_x/CeO_2$ (1.0 g) was added to the THF solution (12 mL, 0.25 M) of NaNaph and stirred vigorously at room temperature for 90 min. The solid was then filtered off, washed with methanol (20 mL) and diethyl ether (20 mL) and dried under an Ar atmosphere to afford 1.0 g of Ni/CeO_2-NaNaph as black powder (Ni content: 1.38 wt%). Various supported nickel catalysts, such as Ni/Al_2O_3-NaNaph (Ni content: 1.25 wt%), Ni/TiO_2-NaNaph (Ni content: 0.85 wt%), Ni/ZrO_2-NaNaph (Ni content: 1.20 wt%) and Ni/HAP-NaNaph (Ni content: 1.39 wt%) were prepared in the same method.

Catalytic reaction

In an Ar-filled glovebox, Ni/CeO_2-NaNaph (3.3 mol%, 40 mg), cyclohexanones (0.3 mmol), *n*-hexadecane (0.1 mmol, internal standard), DMA (2.0 mL), and a Teflon-coated magnetic stir bar were placed into a pressure tube (volume: ~40 mL). The mixture was stirred at 180 °C for 24 h, then the mixture was cooled down to room temperature. Conversions and product yields were determined by GC analysis using *n*-hexadecane as an internal standard. As for isolation of the products, *n*-hexadecane was not added. After the reaction, the catalyst was removed by simple filtration and the filtrate was concentrated by evaporation, and then subjected to silica-gel column chromatography, giving the pure product. The products were identified by GC-MS, and NMR (^1H and ^{13}C).

Data availability

The data generated in this study are provided within the article and its Supplementary Information file. Correspondence and requests for materials should be addressed to K.Y. and T.Y.

References

1 Gao, F., Goodman & D. W. Pd–Au bimetallic catalysts: understanding alloy effects from planar models and (supported) nanoparticles. *Chem. Soc. Rev.* **41**, 8009−8020 (2012).

2 Liu, P. & Nørskov, J. K. Ligand and ensemble effects in adsorption on alloy surfaces. *Phys. Chem. Chem. Phys.* **3**, 3814−3818 (2001).

3 Furukawa, S., Suga, A. & Komatsu, T. Mechanistic study on aerobic oxidation of amine over intermetallic Pd_3Pb: concerted promotion effects by Pb and support basicity. *ACS Catal.* ***5***, 1214−1222 (2015).

4 Wu, D., Baaziz, W., Gu, B., Marinova, M., Hernández, W. Y., Zhou, W., Vovk, E. I., Ersen, O., Safonova, O. V., Addad, A., Nuns, N., Khodakov, A. Y. & Ordomsky, V. V. Surface molecular imprinting over supported metal catalysts for size-dependent selective hydrogenation reactions. *Nat. Catal.* **4**, 595−606 (2021).

5 Kaneda, K. & Mitsudome, T. Metal–Support cooperative catalysts for environmentally benign molecular transformations. *Chem. Rec.* **17**, 4−26 (2017).

6 Sankar, M., He, Q., Engel, R. V., Sainna, M. A., Logsdail, A. J., Roldan, A., Willock, D. J., Agarwal, N., Kiely, C. J. & Hutchings, G. J. Role of the support in gold-containing nanoparticles as heterogeneous catalysts. *Chem. Rev.* **120**, 3890–3938 (2020).

7 Miura, H., Yasui, Y., Masaki, Y., Doi, M. & Shishido, T. Deoxygenative silylation of $C(sp^3)$–O bonds with hydrosilane by cooperative catalysis of gold nanoparticles and solid acids. *ACS Catal*. **13**, 6787–6794 (2023).

8 Jin, X., Tsukimura, R., Aihara, T., Miura, H., Shishido, T. & Nozaki, K. Metal–support cooperation in $Al(PO_3)_3$-supported platinum nanoparticles for the selective hydrogenolysis of phenols to arenes. *Nat. Catal.* **4**, 312−321 (2021).

9 Olah, G. A. Aromatic substitution. XXVIII. mechanism of electrophilic aromatic substitutions. *Acc. Chem. Res.* ***4***, 240–248 (1971).

10 Makosza, M. & Winiarski, J. Vicarious nucleophilic substitution of hydrogen. *Acc. Chem. Res.* **20**, 282−289 (1987).

11 Biffis, A., Centomo, P., Zotto, A. D. & Zecca, M. Pd metal catalysts for cross-couplings and related reactions

in the 21st century: a critical review. *Chem. Rev.* **118**, 2249−2295 (2018).

12 Ley, S. V. & Thomas, A. W. Modern Synthetic Methods for Copper-Mediated C(aryl)−O, C(aryl)−N, and C(aryl)−S Bond Formation. *Angew. Chem. Int. Ed.* **42**, 5400−5449 (2003).

13 Roudesly, F., Oble, J. & Poli, G. Metal-catalyzed C−H activation/functionalization: The fundamentals. *J. Mol. Catal. A* **426**, 275−296 (2017).

14 Izawa, Y., Pun, D. & Stahl, S. S. Palladium-catalyzed aerobic dehydrogenation of substituted cyclohexanones to phenols. *Science* **333**, 209−213 (2011).

15 Dighe, S. U., Juliá, F., Luridiana, A., Douglas, J. J. & Leonori, D. A photochemical dehydrogenative strategy for aniline synthesis. *Nature* **584**, 75−81 (2020).

16 Iosub, A. V. & Stahl, S. S. Palladium-catalyzed aerobic dehydrogenation of cyclic hydrocarbons for the synthesis of substituted aromatics and other unsaturated products. *ACS Catal.* **6**, 8201−8213 (2016).

17 Girard, S. A., Huang, H., Zhou, F., Deng, G.-J. & Li, C.-J. Catalytic dehydrogenative aromatization: an alternative route to functionalized arenes. *Org. Chem. Front.* **2**, 279−287 (2015).

18 Liu, X., Chen, J. & Ma, T. Catalytic dehydrogenative aromatization of cyclohexanones and cyclohexenones. *Org. Biomol. Chem.* **16**, 8662−8676 (2018).

19 Deng, K., Huang, H. & Deng, G.-J. Recent advances in the transition metal-free oxidative dehydrogenative aromatization of cyclohexanones. *Org. Biomol. Chem*. **19**, 6380−6391 (2021).

20 Zhang, J., Jiang, Q., Yang, D., Zhao, X., Dong, Y. & Liu, R. Reaction-activated palladium catalyst for dehydrogenation of substituted cyclohexanones to phenols and H_2 without oxidants and hydrogen acceptors. *Chem. Sci.* **6**, 4674−4680 (2015).

21 Jin, X., Taniguchi, K., Yamaguchi, K. Nozaki, K. & Mizuno, N. A Ni–Mg–Al layered triple hydroxide-supported Pd catalyst for heterogeneous acceptorless dehydrogenative aromatization. *Chem. Commun.* **53**, 5267−5270 (2017).

22 Taniguchi, K., Jin, X., Yamaguchi, K., Nozaki, K. & Mizuno, N. Versatile routes for synthesis of diarylamines through acceptorless dehydrogenative aromatization catalysis over supported gold–palladium bimetallic nanoparticles. *Chem. Sci.* **8**, 2131−2142 (2017).

23 Koizumi, Y., Taniguchi, K., Jin, X., Yamaguchi, K., Nozaki, K. & Mizuno, N. Formal arylation of NH_3 to produce diphenylamines over supported Pd catalysts. *Chem. Commun.* **53**, 10827−10830 (2017).

24 Jin, X., Koizumi, Y., Yamaguchi, K., Nozaki, K. & Mizuno, N. Selective synthesis of primary anilines from cyclohexanone oximes by the concerted catalysis of a Mg–Al layered double hydroxide supported Pd

catalyst. *J. Am. Chem. Soc.* **139**, 13821−13829 (2017).

25 Takayama, S., Yatabe, T., Koizumi, Y., Jin, X., Nozaki, K., Mizuno, N., & Yamaguchi, K. Synthesis of unsymmetrically substituted triarylamines via acceptorless dehydrogenative aromatization using a Pd/C and *p*-toluenesulfonic acid hybrid relay catalyst. *Chem. Sci.* **11**, 4074−4084 (2020).

26 Lin, W.-C., Yatabe, T. & Yamaguchi, K. Selective primary aniline synthesis through supported Pd-catalyzed acceptorless dehydrogenative aromatization by utilizing hydrazine. *Chem. Commun.* **57**, 6530−6533 (2021).

27 Li, H., Yatabe, T., Takayama, S. & Yamaguchi, K. Heterogeneously catalyzed selective acceptorless dehydrogenative aromatization to primary anilines from ammonia via concerted catalysis and adsorption control. *JACS Au* **3**, 1376−1384 (2023).

28 Zeng, G., Shen, L., Zheng, Q. & Tu, T. Selective modular synthesis of *ortho*-substituted phenols via Pd-catalyzed-dehydrogenation−coupling−aromatization of alcohols. *ACS Catal.* **13**, 6222−6229 (2023).

29 Kumar, A., Bhatti, T. M. & Goldman, A. S. Dehydrogenation of alkanes and aliphatic groups by pincer-ligated metal complexes. *Chem. Rev.* **117**, 12357–12384 (2017).

30 Gunanathan, C. & Milstein, D. Applications of acceptorless dehydrogenation and related transformations in chemical synthesis. *Science* **341**, 1229712 (2013).

31 Siddiki, S. M. A. H., Toyao, T., Shimizu, K. Acceptorless dehydrogenative coupling reactions with alcohols over heterogeneous catalysts. *Green Chem.* **20**, 2933−2952 (2018).

32 Zhou, M.-J., Liu, G., Xu, C. & Huang, Z. Acceptorless dehydrogenation of aliphatics, amines, and alcohols with homogeneous catalytic systems. *Synthesis* **55**, 547−564 (2023).

33 Verma, P. K. Advancement in photocatalytic acceptorless dehydrogenation reactions: opportunity and challenges for sustainable catalysis. *Coord. Chem. Rev*. **472**, 214805 (2022).

34 Zhou, M.-J., Zhang, L., Liu, G., Xu, C. & Huang, Z. Site-selective acceptorless dehydrogenation of aliphatics enabled by organophotoredox/cobalt dual catalysis. *J. Am. Chem. Soc*. **143**, 16470−16485 (2021).

35 Fuse, H., Kojima, M., Mitsunuma, H. & Kanai, M. Acceptorless dehydrogenation of hydrocarbons by noble-metal-free hybrid catalyst system. *Org. Lett*. **20**, 2042−2045 (2018).

36 Min, L., Lin, J. & Shu, W. Rapid access to free phenols by photocatalytic acceptorless dehydrogenation of cyclohexanones at room temperature. *Chin. J. Chem*. **41**, 2773−2778 (2023).

37 Jagtap, R. A., Nishioka, Y., Geddis, S. M., Irie, Y., Fuki, M., Kobori, Y., Adachi, R., Yamakata, A., Mitsunuma, A. & Kanai, M. Double hydrogen atom transfer strategy for catalytic acceptorless dehydrogenation of cycloalkanes. Preprint at 10.26434/chemrxiv-2024-s5n5v (2024).

38 Tasker, S. Z., Standley, E. A. & Jamison, T. F. Recent advances in homogeneous nickel catalysis. *Nature* **509**, 299−309 (2014).

39 Chernyshev, V. M. & Ananikov, V. P. Nickel and palladium catalysis: stronger demand than ever. *ACS Catal*. **12**, 1180−1200 (2022).

40 Xu, H., White, P. B., Hu, C. & Diao, T. Structure and isotope effects of the β-H agostic (α-diimine)nickel cation as a polymerization intermediate. *Angew. Chem. Int. Ed.* **56**, 1535−1538 (2017).

41 Xu, H., Hu, C. T., Wang, X. & Diao, T. Structural characterization of β-agostic bonds in Pd-catalyzed polymerization. *Organometallics* **36**, 4099−4102 (2017).

42 Sommer, H., Juliá-Hernández, F., Martin, R. & Marek, I. Walking metals for remote functionalization. *ACS Cent. Sci.* **4**, 153–165 (2018).

43 Li, Y. & Yin, G. Nickel chain-walking catalysis: a journey to migratory carboboration of alkenes. *Acc. Chem. Res.* **56**, 3246–3259 (2023).

44 Juliá-Hernández, F., Moragas, T., Cornella, J. & Martin, R. Remote carboxylation of halogenated aliphatic hydrocarbons with carbon dioxide. *Nature* **545**, 84−88 (2017).

45 Matsuyama, T., Yatabe, T., Yabe, T. & Yamaguchi, K. Heterogeneously catalyzed selective decarbonylation of aldehydes by CeO_2-supported highly dispersed non-electron-rich Ni(0) nanospecies. *ACS Catal*. **11**, 13745−13751 (2021).

46 Matsuyama, T., Yatabe, T. & Yamaguchi, K. Heterogeneously catalyzed decarbonylation of thioesters by supported Ni, Pd, or Rh nanoparticle catalysts. *Org. Biomol. Chem*. **22**, 579−584 (2024).

47 Chen, Y., Qiu, B., Liu, Y. & Zhang, Y. An active and stable nickel-based catalyst with embedment structure for CO_2 methanation. *Appl. Catal. B* **269**, 118801 (2020).

48 Shimizu, K., Kon, K., Shimura, K. & Hakim, S. S. M. A. Acceptor-free dehydrogenation of secondary alcohols by heterogeneous cooperative catalysis between Ni nanoparticles and acid–base sites of alumina supports. *J. Catal.* **300**, 242−250 (2013).

49 Chen, H., He, S., Xu, M., Wei, M., Evans, D. G. & Duan, X. Promoted synergic catalysis between metal Ni and acid–base sites toward oxidant-free dehydrogenation of alcohols. *ACS Catal.* **7**, 2735−2743 (2017).

50 Taniguchi, K., Jin, X., Yamaguchi, K. & Mizuno, N. Facile access to *N*-substituted anilines via dehydrogenative aromatization catalysis over supported gold–palladium bimetallic nanoparticles. *Catal. Sci. Technol.* **6**, 3929−3937 (2016).

51 Takei, D., Yatabe, T., Yabe, T., Miyazaki, R., Hasegawa, J. & Yamaguchi, K. C–H bond activation

mechanism by a Pd(II)–(μ-O)–Au(0) structure unique to heterogeneous catalysts. *JACS Au* **2**, 394−406 (2022).

52 Pun, D., Diao, T. & Stahl, S. S. Aerobic dehydrogenation of cyclohexanone to phenol catalyzed by $Pd(TFA)_2$/2-dimethylaminopyridine: evidence for the role of Pd nanoparticle. *J. Am. Chem. Soc*. **135**, 8213−8221 (2013).

Acknowledgements

This work was financially supported by JSPS KAKENHI Grant No. 21K14460 and 22H04971. This work was supported by JST, PRESTO Grant Number JPMJPR227A, Japan. This work is also based on results obtained from a JPNP20004 project subsidized by the New Energy and Industrial Technology Development Organization (NEDO). We appreciate Dr. Hironori Ofuchi (Japan Synchrotron Radiation Research Institute, SPring-8) for giving great support for XAFS measurements in BL14B2 (proposal no. 2022A1803). A part of this work was conducted at the Advanced Characterization Nanotechnology Platform of the University of Tokyo, supported by "Nanotechnology Platform" of the Ministry of Education, Culture, Sports, Science and Technology (MEXT), Japan. We thank Ms. Mari Morita (The University of Tokyo) for her assistance with the HAADF-STEM and EDS analyses. T.M. was supported by the JSPS through the Research Fellowship for Young Scientists (Grant No. 23KJ0669).

Author contributions

T. Yatabe and K. Y. conceived and supervised the project. T. M. performed most of the experiments. T. Yabe performed the XAFS measurements and analysis. All authors contributed to data analysis and discussed the results. T. M. and T. Yatabe wrote the manuscript with feedback from K. Y. and T. Yabe.

Competing interests

The authors declare no competing financial interests.

Tables

Table 1: Effects of catalysts on the dehydrogenative aromatisation of 4-methylcyclohexanone (1a).[a]

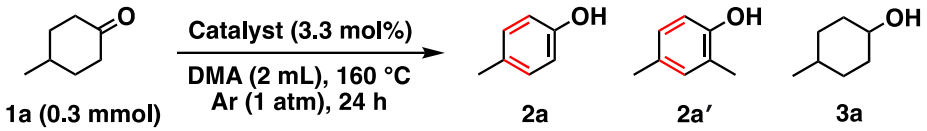

1a (0.3 mmol) — 2a — 2a′ — 3a

Entry	Catalyst	Yield (%)		
		2a	**2a′**	**3a**
1	Ni/CeO_2-0.3NaNaph	50	3	13
2	Cu/CeO_2-0.3NaNaph	1	<1	<1
3	Co/CeO_2-0.3NaNaph	<1	<1	<1
4	Mn/CeO_2-0.3NaNaph	<1	<1	<1
5	Fe/CeO_2-0.3NaNaph	<1	<1	<1
6	Zn/CeO_2-0.3NaNaph	<1	<1	<1
7	Ni/CeO_2-NaNaph	59	6	11
8[b]	Ni/CeO_2-NaNaph	74	13	3
9[b]	Ni/HAP-NaNaph	1	<1	<1
10[b]	Ni/ZrO_2-NaNaph	<1	<1	<1
11[b]	Ni/TiO_2-NaNaph	<1	<1	<1
12[b]	Ni/Al_2O_3-NaNaph	<1	<1	<1
13	CeO_2	<1	<1	<1
14	CeO_2-NaNaph	<1	<1	<1
15	Ni$(OH)_x$/CeO_2	<1	<1	<1
16[c]	Ni/CeO_2-NaNaph	<1	<1	<1
17	Ni/HAP-NaNaph	2	<1	<1
18[d]	Ni/HAP-NaNaph	9	<1	<1
19[e]	Ni/HAP-NaNaph	8	<1	<1
20[b,f]	Ni$(cod)_2$ + IPr	3	<1	<1

[a] Reaction conditions: **1a** (0.3 mmol), catalyst (3.3 mol%), DMA (2 mL), Ar (1 atm), 160°C, 24 h. Yields were determined by GC analysis using *n*-hexadecane as an internal standard. [b] 180°C. [c] PhCOOH (0.3 mmol). [d] CeO_2-NaNaph (40 mg). [e] Na_2CO_3 (0.3 mmol). [f] IPr (6.7 mol%). cod = 1,5-cyclooctadiene. IPr = 1,3-bis(2,6-diisopropylphenyl)imidazol-2-ylidene.